CrossMark

# Green approach to evaluating the thermal hazard reaction of peracetic acid through various kinetic methods

Wei-Chun Chen[1] · Jia-Ru Lin[2] · Min-Siou Liao[2] · Yih-Wen Wang[3] · Chi-Min Shu[4]

**Abstract** Peracetic acid (PAA) is potentially harmful because of its thermal hazards in industrial processes. Attention must be paid to the preparation, manufacturing, transportation, and storage because PAA may readily cause a thermal runaway reaction under various upset scenarios. PAA is classified an explosive substance in the governmental regulation in Taiwan. Here, 20 mass% of PAA was used to estimate the thermokinetic parameters by using differential scanning calorimetry. Heating rates employed were 1.0, 2.0, 4.0, and 8.0 °C min$^{-1}$. We compared the four heating rates of thermal safety assessment with regard to process safety parameters, such as exothermic initial temperature ($T_0$) and heat of decomposition ($\Delta H_d$). Finally, five kinetic analysis methods, along with differential isoconversional kinetic analysis, were used to estimate the apparent activation energy ($E_a$). The experimental results could be used helpful during the manufacturing process, transportation, and storage as the process safety parameter considerations to forestall thermal damage from happening, and to reach zero-disaster purposes as the ultimate goals.

**Keywords** Apparent activation energy · DSC · Peracetic acid (PAA) · Thermal runaways · Thermal safety assessment

## List of symbols

| | |
|---|---|
| $A$ | Frequency factor (s$^{-1}$) |
| $E_a$ | Apparent activation energy (kJ mol$^{-1}$) |
| $f(\alpha)$ | Kinetic functions |
| $k$ | Reaction rate constant (mol L$^{-1}$ s$^{-1}$) |
| $n$ | Reaction order (dimensionless) |
| $n_i$ | Reaction order of $i$th stage (dimensionless) |
| $R$ | Universal gas constant (8.314 J mol$^{-1}$ K$^{-1}$) |
| $T$ | Temperature of reactant (°C) |
| $T_{max}$ | Maximum temperature of reaction (°C) |
| $T_p$ | Peak temperature (°C) |
| $T_0$ | Exothermic onset temperature of reaction (°C) |
| $\Delta H_d$ | Heat of decomposition (J g$^{-1}$) |
| $\alpha$ | Degree of conversion (dimensionless) |
| $\alpha_i$ | Isoconversion degree in various heating rates by Ozawa–Flynn–Wall kinetic equation (dimensionless); $i = 1.0, 2.0, 4.0, 10.0$ |
| $\beta$ | Heating rate (°C min$^{-1}$) |

✉ Chi-Min Shu
  shucm@yuntech.edu.tw

1 Graduate School of Engineering Science and Technology, National Yunlin University of Science and Technology (YunTech), 123, University Rd., Sec. 3, Douliou 64002, Yunlin, Taiwan, ROC

2 Department of Safety, Health, and Environmental Engineering, National Yunlin University of Science and Technology (YunTech), 123, University Rd., Sec. 3, Douliou 64002, Yunlin, Taiwan, ROC

3 Department of Occupational Safety and Health, College of Public Health, China Medical University, 91, Hsueh-Shih Rd., Taichung 40402, Taiwan, ROC

4 Center for Process Safety and Industrial Disaster Prevention, School of Engineering, National Yunlin University of Science and Technology (YunTech), Douliou 64002, Yunlin, Taiwan, ROC

## Introduction

Organic peroxides (OPs) have the functional group –O–O–. Because of this functional group of proxy radicals, OPs are quite unstable and likely to cause thermal catastrophes if not handled properly during the entire process span. Uncontrolled handling of OPs is often accompanied by an

exothermic decomposition reaction, causing severe thermal engendering accidents, such as fire, explosion, and toxic release with subsequent turmoil [1–6].

From 1993 to 2004, four major industrial accidents were caused by peracetic acid (PAA) in the UK. By 2012, PAA had caused a chemical disaster in Shanghai, China. These incidents demonstrate that the thermal instability-related problems of PAA are rather difficult to govern in every operating plant worldwide [7, 8].

PAA, an unstable OP, is classified as an explosive substance with regard to regulations in Taiwan and other Asian countries. Although no major thermal accidents may occur in the manufacturing process, PAA can easily accumulate an enormous amount of heat and also cause an explosion. Equation (1) shows the reversible reaction of PAA. PAA is extremely unstable, and its composition can change any time and reduce rapidly.

$$CH_3COOH + H_2O_2 \overset{H_2SO_4}{\longleftrightarrow} CH_3COOOH + H_2O \qquad (1)$$

We performed a preliminary thermal hazard analysis of PAA through differential scanning calorimetry (DSC). The graphs obtained from experiments show why PAA is fairly hazardous; thus, we should cautiously identify the intrinsic thermal hazard of PAA. In this study, we estimated process safety parameters, such as apparent activation energy ($E_a$), exothermic onset temperature ($T_0$), and heat of decomposition ($\Delta H_d$). After estimating these thermokinetic parameters, differential isoconversional kinetic analysis was employed and five modes of kinetics were deliberately chosen to estimate $E_a$. Through this study, we believe that a prudent operating system could prevent PAA from causing detrimental effects, and the process industry could be well managed and manipulated under an inherently safer design.

## Experimental

### Samples

The structure of PAA is illustrated in Fig. 1. PAA is a colorless liquid, with the typical odor of acetic acid, is a strong oxidizer and strong corrosive agent, and has boiling and flash points of 105.0 and approximately 41.0 °C,
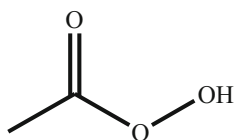
**Fig. 1** Structure of PAA [36, 37]

respectively. PAA can be produced by acetic acid or acetic anhydride with hydrogen peroxide, and sulfuric acid is the catalyst in the reaction. PAA is used as a bleaching agent for pulp and paper, textiles, oils, paraffin, as well as starch. In addition, it is an oxidant and epoxidizing agent in the organic synthesis of compounds, such as propylene oxide, glycerol, synthesis, and glycerin as well as an epoxy plasticizer [9, 10].

### Differential scanning calorimetry

First, we selected the DSC 821$^e$ of Mettler TA8000 system and STAR$^e$ software to obtain basic thermokinetic parameters. Samples were placed in a sealed high-pressure-plated container. DSC tests show the relationship between the changes with temperature of the heat used to measure micro-volume samples, mainly to heat flow type. The experimental thermal heating rates were set at 1.0, 2.0, 4.0, and 8.0 °C min$^{-1}$, along with the range of temperature from 30.0 to 300.0 °C [11–17].

### Thermal activity monitor III

Isothermal calorimetry, thermal activity monitor III (TAM III), was applied to determine the thermal response of the material by using a continuous thermal thermostat system demonstrating high thermal sensitivity and sound stability. The liquid in the TAM III thermostat is mineral oil, which is in a 25-L reactor. Because an external heating thermostat was used, the bottom of the micro-heater has a controlled temper high-pressure-plated container of mineral oil to achieve the perfect isothermal effect. Sample decomposition was then measured using TAM III under isothermal conditions [18, 19]. TAM III software was further used to control the thermostat and calculate some thermokinetic parameters to validate differential isoconversional kinetic analysis as the simulation results. The calculation method by Townsend and Tou is shown in Eq. (2) [20]:

$$\ln(\mathrm{TMR}_{\mathrm{iso}}) = -\ln A + \frac{E_a}{RT} \qquad (2)$$

### Thermal simulations of isoconversional kinetic analysis

Differential isoconversional kinetic analysis was applied to estimate thermal stability under the temperature range and temperature conditions. DSC, differential thermal analysis or thermogravimetry, and experimental data were used, and kinetic parameters were calculated to predict the response mode under isothermal and nonisothermal conditions [21]. Heating rates and baseline curves were acquired, and

kinetic results were obtained from methods of Friedman, Ozawa–Flynn–Wall, ASTM, and Kissinger to define some thermal safety parameters. Otherwise, these methods can also be used to predict the response mode isothermally and nonisothermally and obtain TMR or the limits of experimental conditions.

## Kinetic model simulation

Two possible models of an evaluated decomposition reaction can be used in thermal safety software (TSS) for kinetic analysis. The models can be mainly divided into the $n$th-order reaction and autocatalytic reaction. Therefore, by applying TSS, including TDPro and ForK, the thermokinetic parameters of PAA can be easily confirmed [22, 23]. These data were used to simulate and compare other thermokinetic parameters.

$$N\text{th order reaction:} \quad f(\alpha) = (1 - \alpha)^n \tag{3}$$

$$\text{Autocatalysis reaction:} \quad f(\alpha) = (1 - \alpha)^{n_1}(\alpha^{n_2} + z) \tag{4}$$

## Results and discussion

In general, thermokinetic parameters include exothermic onset temperature ($T_0$), exothermic peak temperature ($T_p$), and heat of decomposition ($\Delta H_d$) under different heating rates. Figure 2 shows the DSC thermal curves of heat flow versus temperature for PAA decomposition at heating rates from 1.0, 2.0, 4.0, to 8.0 °C min$^{-1}$. Two exothermic reactions of PAA appeared during the scanning excursion. The first peak may be causing a self-reacting initial decomposition of PAA at higher temperature or ambient thermal sources, and the second exothermic peak showed
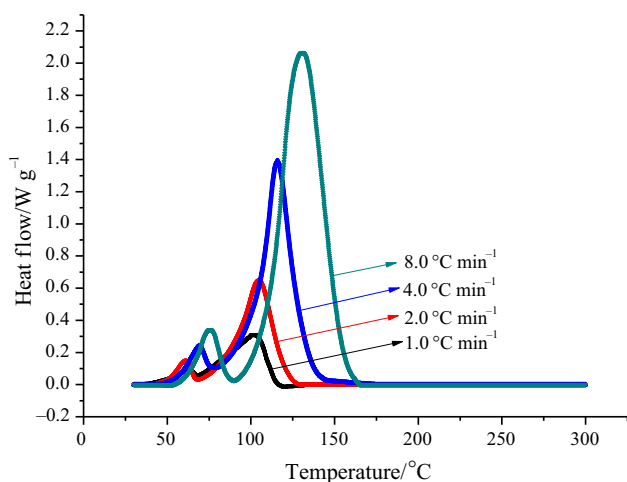


**Fig. 2** DSC thermal curves of heat flow versus temperature for PAA decomposition at heating rates of 1.0, 2.0, 4.0, and 8.0 °C min$^{-1}$

obvious greater extent of thermal intensity under a high-temperature environment, such as in the process operating, storage conditions, or external fire exposure. According to the literatures, PAA has two reaction mechanisms of thermal decomposition. The relative reactivity of radicals with PAA is correlated with the ionization potentials. When the temperature is over 80.0 °C, the free radical will decompose its peroxy acids.

A gradual upward trend of $T_0$ with the heating rate was observed in the experimental results; the thermokinetic parameters obtained by DSC test results are listed in Table 1. The lowest $T_0$ of the four heating rates was approximately 69.4 °C. When the heating rates were increased, $T_0$ was delayed and $T_p$ as well as peak height were increased. Because of the low concentration of PAA, $T_p$ was between 100.0 and 130.0 °C and $\Delta H_d$ was approximately 536.0 J g$^{-1}$, and a low thermal hazard may be possible. Nevertheless, as long as the ambient or operating temperature exceeds 69.4 °C, it could be coupled with thermally unstable conditions, triggering PAA to immediately generate an enormous amount of heat, followed by fire, explosion, and/or chemical release. Compared with our previous studies of organic peroxides, PAA solution is more dangerous than other commercial peroxides in terms of earlier initial exothermal temperature and higher enthalpy.

The isothermal experimental results of heat flow versus time obtained by TAM III are given in Table 2, which presents the thermal behavior of PAA at different isothermal temperatures. The heat flow was increased twofold from 0.011 to 0.022 W g$^{-1}$ at 60.0–70.0 °C. Otherwise, the reaction time would have been over quickly at high experimental temperature. The exothermic curves of PAA occurred earlier along with the various isothermal temperatures at 60.0, 65.0, and 70.0 °C, so that TMR remarkably decreased from 3.3 to 1.3 h, as shown in Fig. 3.

In summary, according to the results from experiments under isothermal conditions, the heat flow was significantly higher at a higher temperature, and TMR was correspondingly smaller.

Five methods were used to calculate $E_a$: Friedman, Ozawa–Flynn–Wall, ASTM E698, Kissinger, and Augis–Bennett analysis [12, 16–21, 24, 25]. $E_a$ is the minimum energy required for a chemical reaction to occur [26–28]. For a complex chemical reaction, $E_a$ varies with the conversion, time, or environmental temperature. Therefore, different step transformations can be obtained to calculate $E_a$ from Friedman and Ozawa–Flynn–Wall methods [12, 20, 21, 24, 25]. $E_a$ was calculated by the estimated function from Friedman, Ozawa–Flynn–Wall, and ASTM E698 methods. The aforementioned five methods were used to calculate $E_a$, and the results derived from the five methods were compared.

**Table 1** Thermokinetic parameters for 20.0 mass% PAA calculated by DSC tests

| Sample | $\beta$/°C min$^{-1}$ | Mass/mg | $T_0$/°C | $T_p$/°C | $\Delta H_d$/J g$^{-1}$ |
|---|---|---|---|---|---|
| 20.0 mass% PAA | 1.0 | 5.2 | 69.4 | 101.3 | 566.9 |
| | 2.0 | 3.6 | 86.6 | 104.9 | 519.0 |
| | 4.0 | 3.2 | 101.0 | 115.9 | 556.4 |
| | 8.0 | 3.6 | 109.0 | 130.7 | 503.6 |

**Table 2** TMR and highest heat flow experimental values and simulation on isothermal thermal curves of heat flow versus time for PAA decomposition at 60.0, 65.0, and 70.0 °C by TAM III

| Temperature/°C | Mass/mg | TMR/h | Highest heat flow/W g$^{-1}$ |
|---|---|---|---|
| 60.0 | 50.1 | 3.28 | 0.011 |
| 65.0 | 50.3 | 1.53 | 0.017 |
| 70.0 | 50.8 | 1.18 | 0.022 |
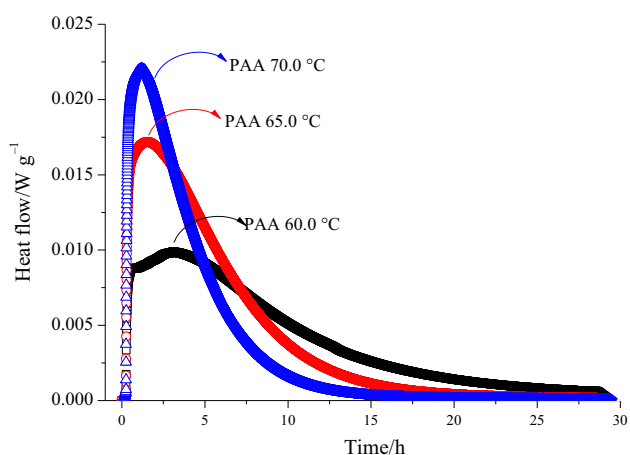


**Fig. 3** TAM III thermal curves of heat flow versus time for PAA decomposition at 60.0, 65.0, and 70.0 °C

At different heating rates, a set of kinetic equations can be derived as follows [17]:

$$\ln\left(\frac{\beta}{T_p - T_0}\right) = \ln(A) - \frac{E_a}{RT_P} \qquad (5)$$

$E_a$ increased along with the enhancement of the reaction progress $\alpha$, indicating that PAA is an easily decomposable chemical and that environmental conditions are a crucial factor for PAA. The minimum $E_a$ was approximately 25.0 kJ mol$^{-1}$, obtained at reaction progress $\alpha$ of approximately 0.1, indicating that PAA was the most hazardous at the incipient stage for this value of reaction progress $\alpha$ according to Friedman [21] (Figs. 4, 5). $E_a$ obtained from the Friedman method was 65.3 kJ mol$^{-1}$. Furthermore, a similar distributed trend was observed for the graphs of ln$k$ versus
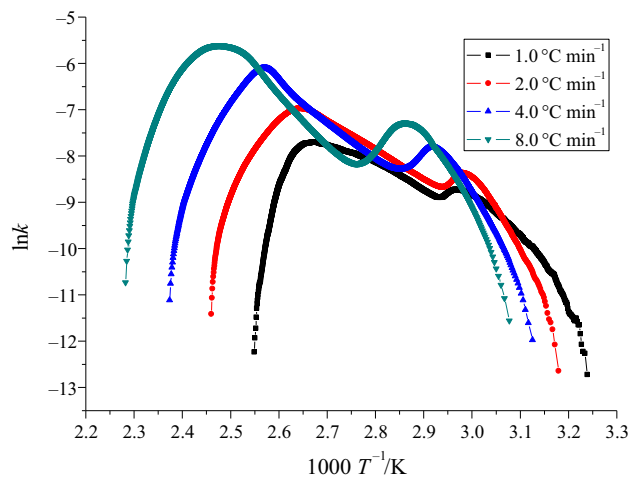


**Fig. 4** Curve fitting of $E(\alpha)$ and ln $A(\alpha)$ by using the Friedman method at heating rates at 1.0, 2.0, 4.0, and 8.0 °C
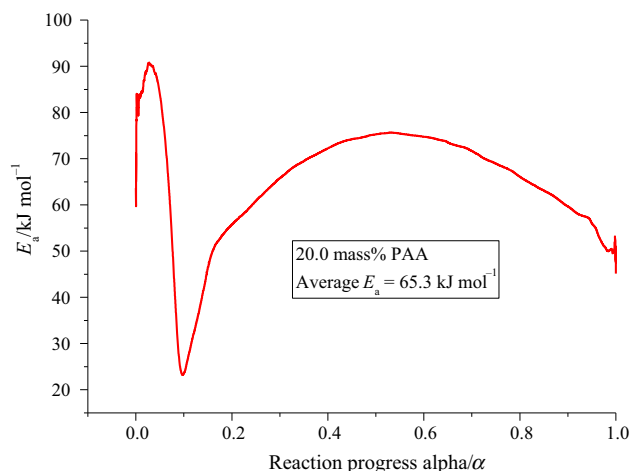


**Fig. 5** Calculation results of $E(\alpha)$ and ln $A(\alpha)$ by using the Friedman method as functions of conversion

$T^{-1}$ at different heating rates (here, 1.0, 2.0, 4.0, 8.0 °C min$^{-1}$), indicating that the heating rate affected the degree of decomposition of PAA, and the decomposition diagram shifted considerably at a high heating rate, as shown in Fig. 4. The aforementioned phenomena of PAA matched the thermal decomposition parameters of general OPs; thus, environmental conditions are a major concern for PAA.

When reaction progress $\alpha$ exceeded 0.05, $E_a$ decreased according to the Ozawa–Flynn–Wall method [12, 21, 24, 25] (Eq. 5). PAA was hazardous even if reaction progress $\alpha$ was 0.2 during the reaction because the $E_a$ of PAA was approximately 55.0 kJ mol$^{-1}$, which is lower than the literature values. Accordingly, the $E_a$ obtained from the Ozawa–Flynn–Wall method was approximately 68.9 kJ mol$^{-1}$. Figure 6 shows that the slopes at reaction progress $\alpha$ of 0.1 and 0.2 are lower than those at other reaction progress $\alpha$ values. A high slope value represents a high $E_a$, because $E_a$ is equal to the product of slope and gas constant. Furthermore, the $E_a$ at reaction progress $\alpha$ of 0.1 had the lowest value, as shown in Fig. 5. Consequently, the $E_a$ distribution diagrams of the Ozawa–Flynn–Wall method have the same trend as those of the Friedman method, because both diagrams shifted obviously at reaction progress $\alpha$ values of 0.1–0.2 (Figs. 5, 6).

The Friedman method is a differential method that can be derived as follows. The Friedman method is displayed as Eq. (6) [21]:

$$k(T) = A'(\alpha) \exp\left[\frac{E_a(\alpha)}{RT}\right] \qquad (6)$$

with $k(T) = \frac{d\alpha}{dt} A'(\alpha) = A'(\alpha) f(\alpha)$.

The Ozawa–Flynn–Wall method can be adopted on the basis of different heating rates under an isoconversional degree condition that is illustrated by Eq. (7) [12, 24, 25, 29–31]:

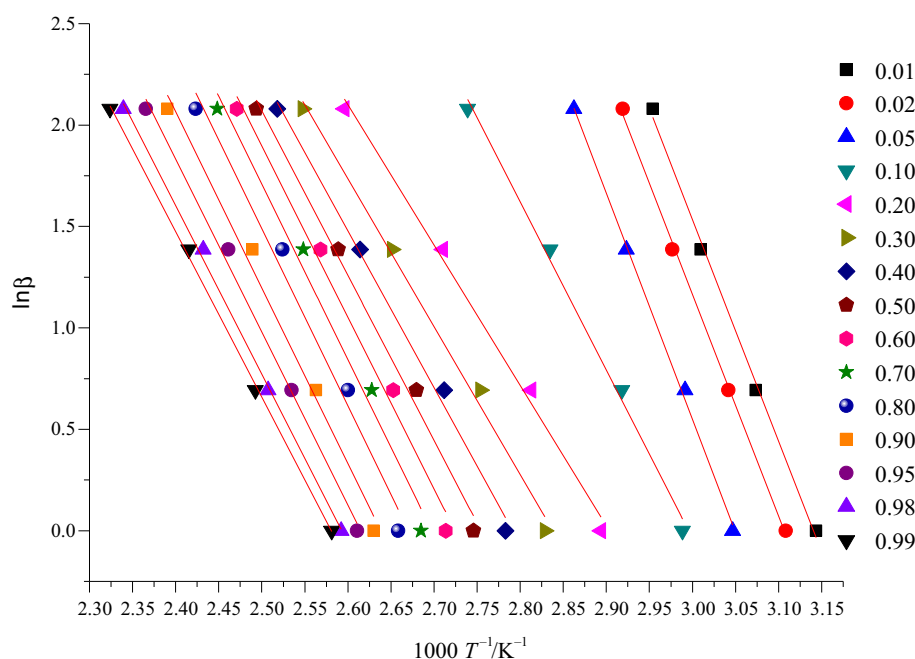$$\ln \beta = -1.0516 \frac{E_a}{RT_{\alpha i}} + \text{const} \qquad (7)$$

Figure 7 shows a diagram developed using ASTM E698, Kissinger, and Augis–Bennett analysis methods [16]. $T_p$ from each heating rate was used in a nonisothermal experiment with four data sets by linear regression. Finally, the slope of the line for each of the four heating rates was $E_a$ of approximately 74.8, 76.4, and 68.1 kJ mol$^{-1}$. In summary of the aforementioned $E_a$ values, which were calculated using the five general thermokinetic methods, the $E_a$ values were almost the same for all the five methods, indicating the correct $E_a$ value of PAA. Finally, we discovered that the $E_a$ value of PAA was extremely low, lower than that of methyl ethyl ketone peroxide (approximately 168.0 kJ mol$^{-1}$), a familiar thermally hazardous material. PAA is more dangerous and difficult to handle in terms of thermal loss prevention [32].

The relationship between the conversion rate and heating rates through the ASTM E698 method is shown by Eq. (8) [16, 33–35], which can be used to determine $E_a(\alpha)$:

$$\ln\left(\frac{\beta}{T_{max}}\right) = \ln\left(\frac{AR}{E_a}\right) + \ln(\alpha_{max}) - \frac{E_a}{RT_{max}} \qquad (8)$$

Based on linear regression, various heating rates and corresponding peak temperatures were obtained. Furthermore, the trend line and slope were used to calculate the $E_a$ as follows in Eq. (9):

$$E_a = \frac{2.303\left[\log\left(\frac{\beta}{T_{max}^2}\right)\right]}{1/T_{max}} \qquad (9)$$

Various heating rates and $T_{max}$ values were acquired using the Kissinger method (Table 4). After putting $T_{max}$
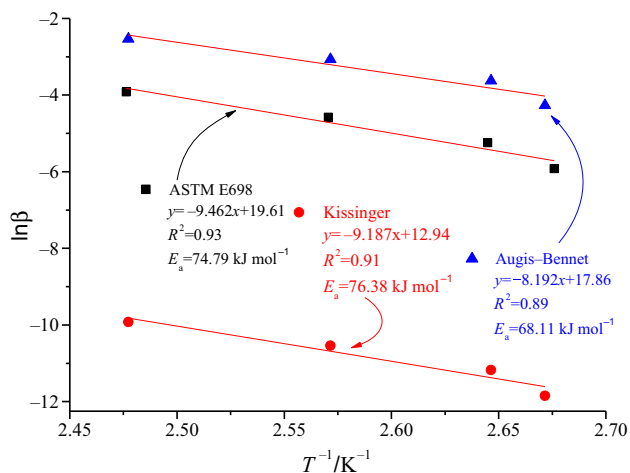


**Fig. 6** Activation energy analysis graph for PAA by the Ozawa–Flynn–Wall method with various conversions

**Fig. 7** Evaluation of $E_a$ by ASTM E698, Kissinger, and Augis–Bennett methods

and heating rates into a natural logarithm function, the value of $E_a$ was approximately 76.4 kJ mol$^{-1}$.

According to these results, the $E_a$ value calculated using the Ozawa–Flynn–Wall method was similar to that in the literature (approximately 70.0 kJ mol$^{-1}$). This finding demonstrated that PAA, during the manufacturing process or transportation, can rapidly generate a large amount of heat in a short time to cause explosion, fire, or gas release.

Figure 8 shows the heat production and heat production rate versus time diagrams. After fitting the results obtained from the five methods, we discovered that $n$th-order reaction along with autocatalytic reaction was obtained by curve fitting and similar thermokinetic parameters were

**Table 3** Activation energy analysis for 20.0 mass% PAA by the Ozawa–Flynn–Wall kinetic equation

| α | Slope | $E_a$/kJ mol$^{-1}$ | Correlation coefficient/$R^2$ |
|---|---|---|---|
| 0.01 | −10.91832 | 86.3 | 0.99634 |
| 0.02 | −10.94374 | 86.5 | 0.99847 |
| 0.05 | −11.13665 | 88.0 | 0.99794 |
| 0.10 | −8.30072 | 65.6 | 0.99309 |
| 0.20 | −6.92054 | 54.7 | 0.99145 |
| 0.30 | −7.28900 | 57.6 | 0.99177 |
| 0.40 | −7.72893 | 61.1 | 0.99260 |
| 0.50 | −8.13421 | 64.3 | 0.99063 |
| 0.60 | −8.45075 | 66.8 | 0.98474 |
| 0.70 | −8.65579 | 68.4 | 0.97860 |
| 0.80 | −8.73677 | 69.1 | 0.98783 |
| 0.90 | −8.67206 | 68.6 | 0.98741 |
| 0.95 | −8.53370 | 67.5 | 0.99412 |
| 0.98 | −8.30787 | 65.7 | 0.99772 |
| 0.99 | −8.15884 | 64.5 | 0.99855 |

**Table 4** Comparison of $E_a$ values for 20.0 mass% PAA obtained by five methods

| Sample | Method | $E_a$/kJ mol$^{-1}$ |
|---|---|---|
| 20.0 mass% PAA | Friedman | 65.3 |
| | Ozawa–Flynn–Wall | 68.9 |
| | ASTM E698 | 74.8 |
| | Kissinger | 76.4 |
| | Augis–Bennett | 68.1 |

**Fig. 8** Heat production versus time and heat production rate versus time of model fitting results of PAA through experiments and simulations with various model approaches
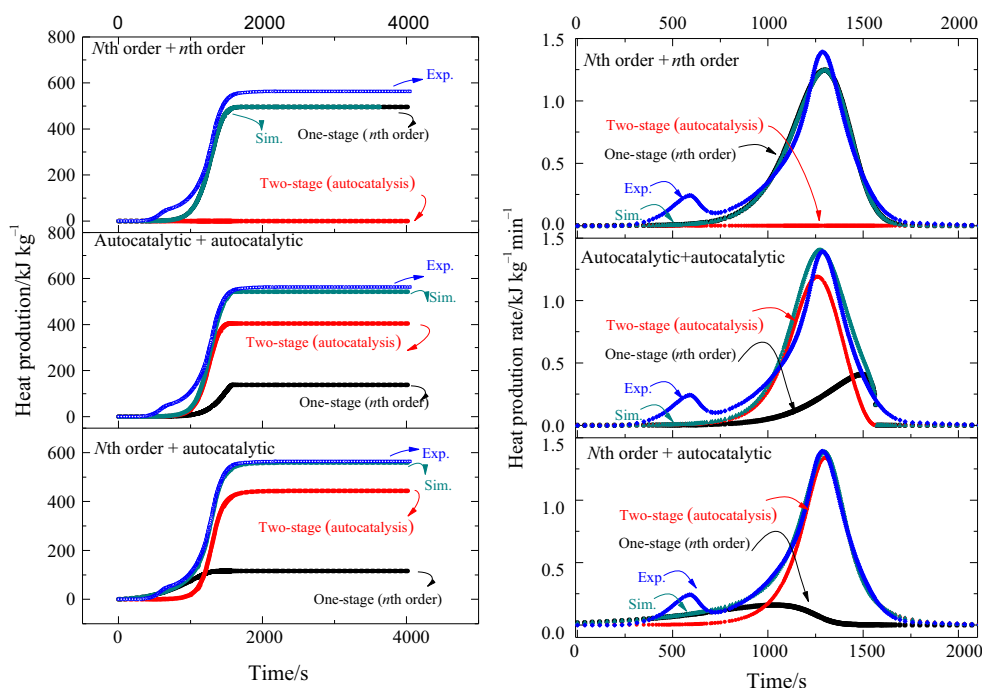
**Table 5** Reaction kinetic simulation for PAA by using a nonlinear regression method

| Kinetics | $N$th order + Autocatalytic | Autocatalytic + Autocatalytic | $N$th order + $n$th order |
|---|---|---|---|
| First stage | $N$th order | Autocatalytic | $N$th order |
| ln ($A$) | 5.2 | 25.5 | 36.5 |
| $E_a$/kJ mol$^{-1}$ | 39.2 | 106.1 | 134.2 |
| Reaction order ($n_1$) | 1.7 | 0.3 | 1.2 |
| Reaction order ($n_2$) | 1.8 | 0.1 | – |
| $\Delta H_d$/kJ kg$^{-1}$ | 500.0 | 424.3 | 495.9 |
| Second stage | Autocatalytic | Autocatalytic | $N$th order |
| ln ($A$) | 19.6 | 18.66 | 12.2 |
| $E_a$/kJ mol$^{-1}$ | 75.0 | 75.0 | 154.9 |
| Reaction order ($n_1$) | 1.7 | 1.7 | 3.0 |
| $\Delta H_d$/kJ kg$^{-1}$ | 577.1 | 599.9 | 249.8 |

obtained for heat production and heat production rate versus time diagrams. Table 3 gives the results from $n$th-order and autocatalytic simulation results. We used $n$th-order reaction (one-stage) combined with autocatalytic reaction (two-stage) fitting for evaluating PAA thermal explosion parameters. Regarding thermal runaway, PAA had two peaks, and a single kinetic model was used to define the kinetic phenomena of the reaction process. We also obtained kinetic parameters through model fitting of the two-stage reaction and comparisons of experimental data and $n$th-order reaction combined with autocatalytic reaction simulated for heat production as well as heat production rate versus time. Therefore, we determined that the decomposition reaction of PAA was a two-stage reaction type that may advance directly to some complex reactions of concern (Tables 4, 5).

## Conclusions

The $T_0$ of PAA is close to the temperature that manufacturers usually choose to boost or initiate a chemical reaction of interest. Thus, PAA is extremely dangerous when being used in processing industries, and it tends to be difficult to manage. According our results, the reaction of PAA decomposed readily because the $E_a$ of PAA was ca. 65.3, 68.9, 74.8, 76.4, and 68.1 kJ mol$^{-1}$ by Friedman, Ozawa–Flynn–Wall, ASTM E698, Kissinger, and Augis–Bennett analyses, respectively. By contrast, the results were different under isothermal temperatures. PAA may have undergone heat accumulation to produce prominent thermal energy because TMR was decreased and the heat flows were increased twofold at the isothermal temperatures for addition. The results revealed that PAA is likely to undergo cleavage and decompose within its chemical

bonds. Accordingly, the operating process must be carefully chosen to avoid unnecessary interference or shutdown. PAA can then be safely handled.

## References

1. Eto I, Akiyoshi M, Miyake A, Ogawa T, Matsunaga T. Hazard evaluation of runaway reaction of hydrogen peroxide-Influence of contamination of various ions. J Loss Prev Process Ind. 2009;22:15–20.
2. Chu YC, Chen WT, Tsai FC, Tsai LC, Lin FR, Shu CM. Evaluation unexpected energy released for three liquid organic peroxides. Energy Educ Sci Tech Pt A. 2012;30:977–82.
3. Jhu CY, Wang YW, Wen CY, Shu CM. Thermal runaway potential of LiCoO$_2$ and Li(Ni$_{1/3}$Co$_{1/3}$Mn$_{1/3}$)O$_2$ batteries determined with adiabatic calorimetry methodology. Appl Energy. 2012;100:127–31.
4. Wang YW, Liao MS, Shu CM. Thermal runaway hazards for LiCoO$_2$ Li-ion batteries by DSC tests. Energy Educ Sci Tech Pt A. 2012;30:1–4.
5. Wang TS, Liu SH, Qian XM, Shu CM. Isothermal hazards evaluation of benzoyl peroxide mixed with benzoic acid via TAM III test. J Therm Anal Calorim. 2013;113:1625–31.
6. Lin JR, Liao MS, Wang YW, Jhu CY, Liu SH, Shu CM. Thermal hazard evaluations of peracetic acid by DSC and AKTS. In: Proceedings of the 6th international conference on process systems engineering (PSE ASIA) 25-27 June 2013, Kuala Lumpur, Malaysia.
7. OSH-ROM, Major harzard incident data service (MHIDAS). Health and Safety Commission (HSC), UK.
8. Wang YW, Liao MS, Shu CM. Thermal hazards of a green antimicrobial peracetic acid combining DSC calorimeter with thermal analysis equations. J Therm Anal Calorim. 2015;119(3):2257–67.
9. Baldry MGC. The bactericidal, fungicidal and sporicidal properties of hydrogen peroxide and peracetic-acid. J Appl Bacteriol. 1983;54:417–23.

10. Kitis M. Disinfection of wastewater with peracetic acid: a review. Environ Int. 2004;30:47–55.

11. Hou HY, Liao TS, Duh YS, Shu CM. Thermal hazard studies for dicumyl peroxide by DSC and TAM. J Therm Anal Calorim. 2006;83:167–71.

12. Lee MH, Chen JR, Shiue GY, Lin YF, Shu CM. Simulation approach to benzoyl peroxide decomposition kinetics by thermal calorimetric Technique. J Taiwan Inst Chem E. 2014;45:115–20.

13. Li AC, Tsai YT, Wu SH, Chiu CW, Shen SJ, Hsin R, Shu CM. Thermal runaway analysis for two organic peroxides with $H_2O$ and dry fire-extinguishing chemicals by DSC and VSP2. J Therm Anal Calorim. 2013;113:1611–8.

14. Liu SH, Hou HY, Shu CM. Effects of thermal runaway hazard for three organic peroxides conducted by acids and alkalines with DSC, VSP2, and TAM III. Thermochim Acta. 2013;566:226–32.

15. Weng SY, Liu SH, Tsai LC, Hsieh TF, Ma CM, Shu CM. Thermokinetics simulation for multi-walled carbon nanotubes with sodium alginate by advanced kinetics and technology solutions. J Therm Anal Calorim. 2013;113:1603–10.

16. Zang N, Qian XM, Liao JY, Shu CM. Thermal stability of lauroyl peroxide by isoconversional kinetics evaluation and finite element analysis. J Taiwan Inst Chem E. 2014;45:461–7.

17. Augis JA, Bennett JE. Calculation of the Avrami parameters for heterogeneous solid-state reactions using a modification of the Kissinger method. J Therm Anal Calorim. 1978;13:283–92.

18. Product Information, TAM III Thermostat. www.thermometric.com. 2014.

19. Tseng JM, Liu MY, Chen SL, Hwang WT, Gupta JP, Shu CM. Runaway effects of nitric acid on methyl ethyl ketone peroxide by TAM III test. J Therm Anal Calorim. 2009;96:789–93.

20. Townsend DI, Tou JC. Thermal hazard evaluation by an accelerating rate calorimeter. Thermochim Acta. 1980;37:1–30.

21. AKTS AG. AKTS-thermokinetics software and AKTS-thermal safety software. http://www.akts.com. (2015).

22. ASTM International. ASTM standard E698, standard test method for Arrhenius kinetic constants for thermally unstable materials using differential scanning calorimetry and the Flynn/Wall/Ozawa method, West Conshohocken, PA, USA. 2013.

23. ChemInform Saint-Petersburg (CISP) Ltd. Thermal Safety Software (TSS). http://www.cisp.spb.ru/.

24. Käser F, Roduit B. Prediction of the ageing of rubber using the chemiluminescence approach and isoconversional kinetics. J Therm Anal Calorim. 2008;93:231–7.

25. Friedman HL. Kinetics of thermal degradation of char-forming plastics from thermogravimetry. Application to a phenolic plastics. J Polym Sci Part C: Polym Symp. 1964;6:183–95.

26. Lin CP, Chang CP, Chou YC, Chu YC, Shu CM. Modeling solid thermal explosion containment on reactor HNIW and HMX. J Hazard Mater. 2010;176:549–58.

27. Dellavedova M, Pasturenzi C, Gigante L, Lunghi A. Kinetic evaluations for the transportation of dangerous chemical compounds. Chem Eng Trans. 2012;26:585–90.

28. Flynn JH, Wall LA. General treatment of the thermogravimetry of polymers. J Res Nat Bur Stand. 1966;70A:487–523.

29. Ozawa T. Kinetic analysis of derivative curves in thermal analysis. J Therm Anal Calorim. 1970;2:301–24.

30. Ozawa T. Estimation of activation energy by isoconversion methods. Thermochim Acta. 1992;203:159–65.

31. Ozawa T. Thermal analysis-review and prospect. Thermochim Acta. 1999;355:35–42.

32. Wu SH, Su CH, Shu CM. Thermal accident investigation of methyl ethyl ketone peroxide by calorimetric technique. Int J Chem Sc. 2008;6:487–96.

33. American Society for Testing and Materials (ASTM). E698 Standard test method for Arrhenius kinetic constants for thermally unstable materials. West Conshohocken, PA, USA. 2001.

34. Ozawa T. A new method of analyzing thermogravimetric data. Bull Chem Soc Jpn. 1965;38:1881–7.

35. Flynn JH, Wall LA. A quick, direct method for the determination of activation energy from thermogravimetric data. J Polym Sci B. 1966;4(5):323–8.

36. Koubek E, Haggett ML, Battaglia CJ, Ibne-Rasa KM, Pyun HY, Edwards JO. Kinetics and mechanism of the spontaneous decompositions of some peroxyacids, hydrogen peroxide and t-butyl hydroperoxide. J Am Chem Soc. 1963;85:2263–8.

37. Yuan Z, Ni Y, Heiningen V. Kinetics of peracetic acid decomposition. Part I: spontaneous decomposition at typical pulp bleaching conditions. Can J Chem Eng. 1997;75(1):37–41.